

Toll-Like Receptor Expression and Activation in Mice with Experimental Dry Eye

Rachel L. Redfern,¹ Nimesh Patel,¹ Samuel Hanlon,¹ William Farley,² Margaret Gondo,¹ Stephen C. Pflugfelder,² and Alison M. McDermott¹

PURPOSE. To investigate the expression and/or function of toll-like receptors (TLRs) and antimicrobial peptides (AMPs) in dry eye inflammation.

METHODS. Experimental dry eye (EDE) was induced in C57BL/6 mice and TLR mRNA and protein expression were determined at the ocular surface and lacrimal gland. TLR agonist cocktail was applied to the ocular surface in untreated (UT), corneal scratched, and EDE mice. The corneal expression of cathelin-related antimicrobial peptide (CRAMP; human LL-37 orthologue), and mouse beta defensin (mBD)-3 and -4 (human BD-2 orthologue) was compared. LL-37, hBD-2, TLR4, 5, and TLR9 mRNA expression was examined in patients with dysfunctional tear syndrome (DTS) via conjunctival impression cytology. Murine central corneal thickness (CCT) and inflammatory cell recruitment into the stroma was determined by in vivo imaging.

RESULTS. EDE upregulated TLR2-4 and 9 mRNA expression in the palpebral conjunctiva and with the exception of TLR4, a similar expression, occurred in the corneal epithelium. TLR2 and 5 were upregulated in lacrimal gland and overall, there was a corresponding change in TLR protein. EDE decreased CRAMP mRNA and protein. hBD-2 and TLR9 expression were modulated in DTS subjects. Topical TLR agonist increased inflammatory cells recruitment and CCT in mice with a cornea scratch. In EDE, TLR agonist treatment downregulated corneal mBD-4 protein caused corneal epithelial loss, and stromal ulceration resulting in decreased CCT.

CONCLUSIONS. DTS modulates the expression of TLR and CRAMP and topical application of TLR agonists in EDE mice resulted in corneal epithelial loss and thinning. These results suggest that TLRs are involved in DTS inflammation. (*Invest Ophthalmol Vis Sci.* 2013;54:1554-1563) DOI:10.1167/iovs.12-10739

Dysfunctional tear syndrome (DTS) or dry eye is a common multifactorial inflammatory condition that results in ocular discomfort and patients are three times more likely to

report problems with common daily activities.¹ Although the pathogenesis is not fully understood, DTS inflammation is thought to be driven by tear film hyperosmolarity²⁻⁴ and instability, which leads to an increase in proinflammatory cytokines⁵⁻⁷ and matrix metalloproteinases (MMPs)⁸ at the ocular surface. In dry eye, the ocular surface epithelium is often compromised and prone to ulceration,⁹ the risk for microbial infection would appear to be increased in these patients.¹⁰ However, this is not often reported in the literature and few data exist on the risk of infection in DTS.

The ability of the ocular surface to mount an immune response to infectious pathogens is in part attributed to toll-like receptors (TLRs) and antimicrobial peptides (AMPs), and a change in their expression may alter the risk for infection. TLR activation triggers the production of various proinflammatory cytokines, chemokines, and AMPs commonly found on the ocular surface. In the human and mouse corneal and conjunctival epithelial cells, human β -defensins (hBD)-1 and -3 and cathelicidin (LL-37) are expressed, while hBD-2 expression is inducible by conditions mimicking injury, inflammation and in response to bacterial products.¹¹⁻¹⁴

TLRs are expressed on ocular surface cells in humans,¹⁵ and in the mouse,¹⁶ and recognize and respond to various microbes and endogenous stress ligands. It has been proposed that TLRs are involved in DTS inflammation. TLR1, 2, and 4¹⁷ and TLR2-4¹⁸ expression are increased in salivary cells and glands from Sjogren's Syndrome (SS) patients, respectively, suggesting their active participation in SS inflammation. In such a scenario, it is envisioned that TLR activation is most likely via various endogenous ligands and/or normal flora bacteria rather than pathogens. For example, an increase in the number of TLRs may lead to TLR over activation, but also an increase the production of AMPs to reduce the risk of microbial infections. Therefore, determining if TLR and AMP expression is modulated in DTS may provide insight into the pathogenesis of the disease and the risk for microbial infections. In this study, the expression of TLRs and antimicrobial peptides were examined in mice with experimental dry eye (EDE) and in DTS patients. To determine if mice with EDE are more susceptible to TLR-induced inflammation than normal mice, a one-time dose of TLR agonist cocktail was applied to the ocular surface and the corneal inflammatory response was examined by in vivo imaging and immunohistochemistry.

METHODS

Experimental Dry Eye Mouse Model

This research protocol was approved by the Institutional Animal Care and Use Committee and conformed to the standards in the ARVO Statement for the Use of Animals in Ophthalmic and Vision Research. EDE was induced in 6- to 12-week-old C57BL/6 mice (The Jackson Laboratory, Bar Harbor, ME) as previously reported¹⁹ for 5 days (5D). In

From the ¹University of Houston, College of Optometry, Houston, Texas; and the ²Department of Ophthalmology, Baylor College of Medicine, Ocular Surface Center, Cullen Eye Institute, Houston, Texas.

Supported by Grants EY13175 (AMM), EY07024 and EY18113 (RLR), EY007551 (University of Houston College of Optometry, CORE grant), and a William C. Ezell Fellowship from the American Optometric Foundation (RLR).

Submitted for publication August 9, 2012; revised November 28, 2012 and January 4, 2013; accepted January 21, 2013.

Disclosure: **R.L. Redfern**, None; **N. Patel**, None; **S. Hanlon**, None; **W. Farley**, None; **M. Gondo**, None; **S.C. Pflugfelder**, None; **A.M. McDermott**, None

Corresponding author: Rachel L. Redfern, College of Optometry, University of Houston, 505 J. Davis Armistead Building, 4901 Calhoun Road, Houston, TX 77204-2020; redfern.rachel@gmail.com.

age- and sex-matched mice that did not receive any treatment to induce EDE served as the untreated (UT) control. After 5D of treatment, the animals were euthanized and the corneal epithelium was removed by scraping and the conjunctiva and lacrimal gland were removed by dissection and placed in tubes containing denaturation solution (ToTALLY RNA kit; Ambion, Austin, TX) and snapped frozen. The samples were stored at -80°C until further analysis to determine TLR2-5, TLR9, CRAMP, mBD-3-4 mRNA expression (5 animals/group, $n = 3-4$). In another set of animals, whole eyes were removed for immunohistochemistry to determine TLR2-5, CRAMP, mBD-3, and mBD-4 protein expression ($n = 2$).

Scratch Model

Six- to 12-week-old C57BL/6 mice of both sexes (Jackson Laboratories) were anesthetized by intraperitoneal injection (ketamine, 60 mg/kg; xylazine 6 mg/kg; Vedco, Inc., St. Joseph, MO). Using a surgical microscope, three parallel 1-mm scratches were made to both eyes using a sterile 27-gauge needle as previously described.²⁰

Topical Application of TLR Agonist Cocktail

To evaluate the role of TLR agonists in EDE inflammation, C57BL/6 mice were divided into three treatment groups: (1) UT control mice, n equals 6 (negative control), (2) EDE mice, n equals 8, and (3) scratch (positive control), n equals 3. Mice were manually restrained and a one-time topical application of 5 μL of vehicle control (endotoxin-free physiological water) was applied to the left eye or 5 μL of TLR agonist cocktail was applied to the right eye. To prepare the cocktail, individual mouse TLR agonists (Invivogen, San Diego, CA) were reconstituted in endotoxin-free physiologic water, then combined to give final concentrations of TLR2 agonist: Pam3CSK3 (1 $\mu\text{g}/\mu\text{L}$), TLR3 agonist: PolyI:C (1 $\mu\text{g}/\mu\text{L}$), TLR5 agonist: Flagellin (1 $\mu\text{g}/\mu\text{L}$), and TLR9 agonist: ODN M362 (4 $\mu\text{g}/\mu\text{L}$). Following instillation of drops, the animals were returned to the vivarium (UT or scratch mice) or continued EDE treatment. In vivo images (see below) were taken 24 hours post stimulation, then the mouse was euthanized and the entire eye removed and processed for either immunostaining for CRAMP, mBD-3, and mBD-4, or paraffin embedded for histologic analysis.

Human Subjects

All procedures involving human subjects were in accordance with the tenets of the Declaration of Helsinki and were approved by the University of Houston institutional review board. Written informed consent was obtained from all subjects before participating in the study. Subjects were screened and categorized as healthy or DTS by their subjective responses of the ocular surface disease index (OSDI) questionnaire²¹ and the presence of objective clinical signs were also compared between DTS and healthy subjects. Corneal and conjunctival epithelial staining (graded 1-4 as per Cornea and Contact Lens Research Unit grading scale with fluorescein and lissamine green, respectively; School of Optometry, University of New South Wales, Sydney, Australia), tear production (phenol red thread test), tear film osmolality (vapor pressure osmometer, Vapro 5520; Wesco, Inc., Logan, UT); and tear stability (fluorescein tear break-up time, Dry Eye Test; Akorn, Chicago, IL) were obtained.

Conjunctival Impression Cytology

Following the completion of all the objective clinical assessments, a single drop of 0.5% proparacaine hydrochloride anesthetic (Bausch and Lomb, Rochester, NY) was instilled onto the eyes. Two to three 6.5×13 mm sterile polyether sulfone membranes (Supor; Pall Gellman Sciences, East Hills, NY) were placed on the superior or inferior bulbar conjunctiva without applying pressure on each eye. The membranes were removed from both eyes and placed directly in one tube containing 350 μL of lysis buffer (Qiagen, Valencia, CA) and stored at

-80°C until further RT-PCR analysis for hBD-2 and hCAP-18 (LL-37 precursor) mRNA expression. Total RNA from conjunctival impression cytology (CIC) samples was extracted using an RNeasy Micro Kit (Qiagen). RNA elution columns were treated with DNase prior to RNA extraction to avoid genomic DNA contamination

Immunohistochemistry

Following in vivo imaging, the eyes including the lids of mice were excised, embedded in optimal cutting temperature (OCT) compound (VWR, Suwanee, GA), and frozen in liquid nitrogen. Sagittal 10- μm sections were cut with a cryostat (Leica CM 1950; Leica, Bannockburn, IL) and placed on glass slides and stored at -80°C . Sections were fixed with acetone and placed in blocking solution (0.1% of goat or rabbit serum, 0.1% Triton X-100, 1% fish gelatin, and 5% BSA). After blocking for 2 hours, the sections were incubated with 1 $\mu\text{g}/\text{mL}$ of either goat anti-CRAMP, rabbit anti-mBD-3, rabbit anti-mBD-4 (Santa Cruz Biotechnology, Santa Cruz, CA), 10 $\mu\text{g}/\text{mL}$ anti-TLR2 (Abcam, Cambridge, MA), 10 $\mu\text{g}/\text{mL}$ anti-TLR3 (Imgenex, San Diego, CA), 5 $\mu\text{g}/\text{mL}$ anti-TLR4 (Abcam), or 10 $\mu\text{g}/\text{mL}$ anti-TLR5 (Imgenex), at 4°C overnight. The following morning, slides were washed in PBS and blocked again for 30 minutes at room temperature and then incubated with the respective (5 $\mu\text{g}/\text{mL}$) Alexa 546- or (6.6 $\mu\text{g}/\text{mL}$) Alexa 488-conjugated second antibody (Invitrogen, Grand Island, NY) in blocking solution for 1 hour at room temperature in the dark. As a negative control, some sections were incubated with the same concentration of a relevant isotype control instead of the primary antibody. Coverslips were mounted with ProLong Gold antifade reagent with 4,4'-diamidino-2-phenylindole (DAPI; Invitrogen) and the sections were visualized with the same exposure time using a DeltaVision imaging system (Applied Precision, Issaquah, WA)

Real-Time PCR

cDNA was generated using SuperScript III First-Strand Synthesis System (Invitrogen). Reverse transcription was performed at 50°C for 60 minutes. Samples containing no reverse transcriptase or water in place of RNA (no template control) served as negative controls. PCR amplification of cDNA was performed with Brilliant SYBR Green QPCR Master Mix (Stratagene, La Jolla, CA) using specific primers listed in the Table. Thermocycle parameters for these primers were 95°C for 10 minutes, followed by amplification of cDNA for 40 cycles by denaturation 95°C for 30 seconds, annealing 58°C for 60 seconds, and extension 72°C for 30 seconds. To examine mouse TLR4 mRNA expression, FAM labeled Taqman primers (Applied Biosystems, Carlsbad, CA) were used (mouse TLR4:Mn00445273 and mouse glyceraldehyde 3-phosphate dehydrogenase [GAPDH]:Mn03302249) using thermocycler parameters of 95°C for 10 minutes, followed by amplification of cDNA for 40 cycles of denaturation 95°C for 15 seconds, annealing and extension at 60°C for 60 seconds. All reactions were done in triplicate using an Mx3005P QPCR System (Stratagene). Amplified gene products were normalized to GAPDH or RNA polymerase II (RPII), the internal control and calibrated to untreated control samples. The relative change of treated versus control samples was then determined with the value of control samples being normalized to one. Disassociation melt curves were analyzed to ensure reaction specificity. Data are representative of a minimum of two to three experiments. Data were first analyzed with a one way ANOVA and then Student's t -test where P less than or equal to 0.05 was considered a significant difference.

Spectralis Spectral Domain Optical Coherence Tomography

The SD-OCT instrument (Heidelberg Engineering, Heidelberg, Germany) was used to evaluate the corneal epithelial integrity and central corneal thickness (CCT) in UT mice ($n = 6$) and mice subjected to EDE ($n = 8$). Following treatment, mice were anesthetized and a sodium

TABLE. Primer Sequences Used with SYBR Green Analysis

Primer Name	Sequence (5'-3')
hGAPDH	Forward: GACCACAGTCCATGCCATCA
hGAPDH	Reverse: CATCACGCCACAGTTTCC
hBD-2	Forward: GACTCAGCTCCTGGTGAAGC
hBD-2	Reverse: TTTTGTTCAGGGAGACCAC
LL-37	Forward: GGACAGTGACCCTCAACCAG
LL-37	Reverse: AGAAGCCTGAGCCAGGGTAG
mTLR2	Forward: CGTTGTTCCTGTGTTGCT
mTLR2	Reverse: AAAGTGGTTGTGCGCTGCT
mTLR3	Forward: TTGCGTTGCCAAGTGAAG
mTLR3	Reverse: TAAAAAGAGCGAGGGGACAG
mTLR5	Forward: CAGGATGTTGGCTGGTTTCT
mTLR5	Reverse: CGGATAAAGCGTGGAGAGTT
mRPII	Forward: CTACACCACCTACAGCTCCAG
mRPII	Reverse: TTCAGATGAGGTCATGAGGAT
CRAMP	Forward: GCCGCTGATTCCTTTTGACAT
CRAMP	Reverse: GCCAAGGCAGGCTACTACT
mBD-3	Forward: GGATCCATTACCTTCTGTTTGC
mBD-3	Reverse: ATTYGAGGAAAGGAACCTCCAC
mBD-4	Forward: GCTTCAGTCATGAGGATCCAT
mBD-4	Reverse: CTTGCTGGTTCCTTCGTCCTTTT

fluorescein strip (Ful-Glo; Akorn, Lake Forest, IL) wet with preservative-free saline (Unisol; Alcon, Fort Worth, TX) was applied to the ocular surface and corneal staining examined using 488 nm wavelength blue light illumination. To evaluate the fluorescein staining intensity, images were analyzed using NIH ImageJ software. The fluorescein staining was graded in the central cornea using a 1-mm diameter circle. The grayscale was converted to a black and white binary detection scale and the same detection threshold was used to analyze each image. The number of black pixels (fluorescein stained sections of the cornea) were counted and averaged for the right and left eye of each group. In vivo CCT was determined as previously described.²² Images were analyzed using ImageJ software and an appropriate pixel to length (μm) conversion factor was applied. Data were analyzed using a Student's *t*-test where *P* less than or equal to 0.05 was considered a significant difference compared with the UT control group.

In Vivo Imaging Using Heidelberg Retinal Tomography (HRT) III

HRT III Rostock Corneal Module (Heidelberg Engineering) was used to investigate the corneal inflammatory response using enface and oblique sectional images similar to that as previously described.²³ The objective lens was covered with a TomoCap (Heidelberg Engineering) and Genteel (Novartis, Basel, Switzerland) was placed on the tip of the objective lens and the cap to maintain immersion contact between the lens and the eye. Animals were positioned so that the corneal apex was perpendicular to the objective cap. Oblique sections and enface images were taken with a 400- μm objective lens, covering an area of $400 \times 400 \mu\text{m}$ and were acquired using an automatic-gain mode. Corneal images were taken from the apex of the cornea and oblique sections of the peripheral cornea were obtained by focusing up to a depth of 700 μm . Enface images 5 to 10 μm beneath the basal epithelium were identified as previously described²⁴ and evaluated using a volume scan.

Paraffin Embedding and Hematoxylin and Eosin Staining

Following in vivo imaging, whole mouse eyes were immediately dissected and placed in 10% neutral buffered formalin (NBF). The tissue was processed using the Pelco Biowave Pro Microwave

Processor and the Pelco ColdSpot Pro (Ted Pella, Inc., Redding, CA). Briefly, whole eyes were processed in NBF for 45 minutes at 150 Watts (W) and then for 5 minutes at 650 W. The tissue was gradually dehydrated using four graded changes of ethanol (70%, 95%, and 100%) at 150 W for 5 minutes each and then cleared using 100% xylene and processed for 10 minutes at 250 W and 650 W. The tissues were impregnated with three changes of paraffin (Leica Microsystems, Buffalo Grove, IL), at 650 W for 10 minutes with each change. The tissue was then blocked, cut in 10- μm sagittal sections using a Leica 2235 Rotary Microtome and stained with Mayer's Hematoxylin and Eosin (H&E).

RESULTS

TLR Expression Is Upregulated on the Ocular Surface and Lacrimal Gland in Mice with EDE

C57BL/6 mice were subjected to EDE for 5D and then expression of TLR2-5 and TLR9 mRNA was compared with that of UT control mice by real-time PCR (Fig. 1A). One way ANOVA revealed a statistically significant difference in TLR expression between UT and EDE mice in the cornea F(5, 16.14) equals 8.108, *P* equals 0.002, conjunctiva F(5, 244.5) equals 5.745, *P* equals 0.004, and lacrimal gland F(5, 102) equals 16.72, *P* less than or equal to 0.001. In the corneal epithelium of EDE mice, there was a significant upregulation in TLR2, 3, 5, and TLR9 mRNA expression by 2.5 ± 0.3 -, 3.8 ± 1.4 -, 2.2 ± 0.2 -, and 2.2 ± 0.3 -fold, respectively. However, there was no significant change in TLR4 expression (1.1 ± 0.1 -fold) compared with the UT control mice. In the conjunctiva, all TLRs mRNA were upregulated with TLR2, 3, 4, 5, and 9 being upregulated by 2.5 ± 0.4 -, 9.0 ± 5.1 -, 8.3 ± 5.3 -, 3.8 ± 2.0 -, and 6.7 ± 4.1 -fold, respectively. In the lacrimal gland, TLR4 and TLR9 were downregulated by 0.4 ± 0.02 - and by -1.3 ± 0.5 -fold, respectively, while TLR2 was upregulated by 6.0 ± 1.4 -fold and TLR5 by 6.1 ± 1.0 -fold. There was no significant change in TLR3 (2.6 ± 2.1 -fold change).

Immunohistochemistry was also performed to examine TLR2-5 protein. In the corneal epithelium and palpebral conjunctiva there were increases in TLR2, 3, and 5 (Figs. 1B, 1C). In the lacrimal gland there was a striking increase in TLR5 protein and a modest increase in TLR2 and TLR3 (Fig. 1D). There was no distinguishable difference in TLR4 in the EDE and UT mice in all samples tested. There was no detectable TLR9 signal above background despite trying antibodies from different suppliers at various concentrations.

EDE and TLR Activation Modulates the Expression of Antimicrobial Peptides (AMPs) on the Ocular Surface

C57BL/6 mice were subjected to EDE for 5D and then expression of AMPs mRNA was compared with that of UT control mice by real-time PCR (Fig. 2A). One way ANOVA revealed a statistically significant difference in AMPs expression between UT and EDE mice in the cornea F(3, 7.858) equals 5.201, *P* equals 0.028. Real-time PCR (Fig. 2A) revealed that in the corneal epithelium CRAMP (LL-37 orthologue) mRNA was significantly downregulated by 0.8 ± 0.3 -fold, while mBD-3 and mBD-4 (hBD-2 orthologue) were upregulated although this did not reach statistical significance ($n = 3$). Immunostaining (Fig. 2B) revealed a decrease in CRAMP but no change in mBD-3 or -4 protein ($n = 2$). In a separate experiment, mice were subjected to EDE and then a one-time topical application of a TLR agonist cocktail (TLR2, 3, 5, 9) or the endotoxin-free vehicle control. These specific TLR agonists were chosen since they were upregulated in the corneal

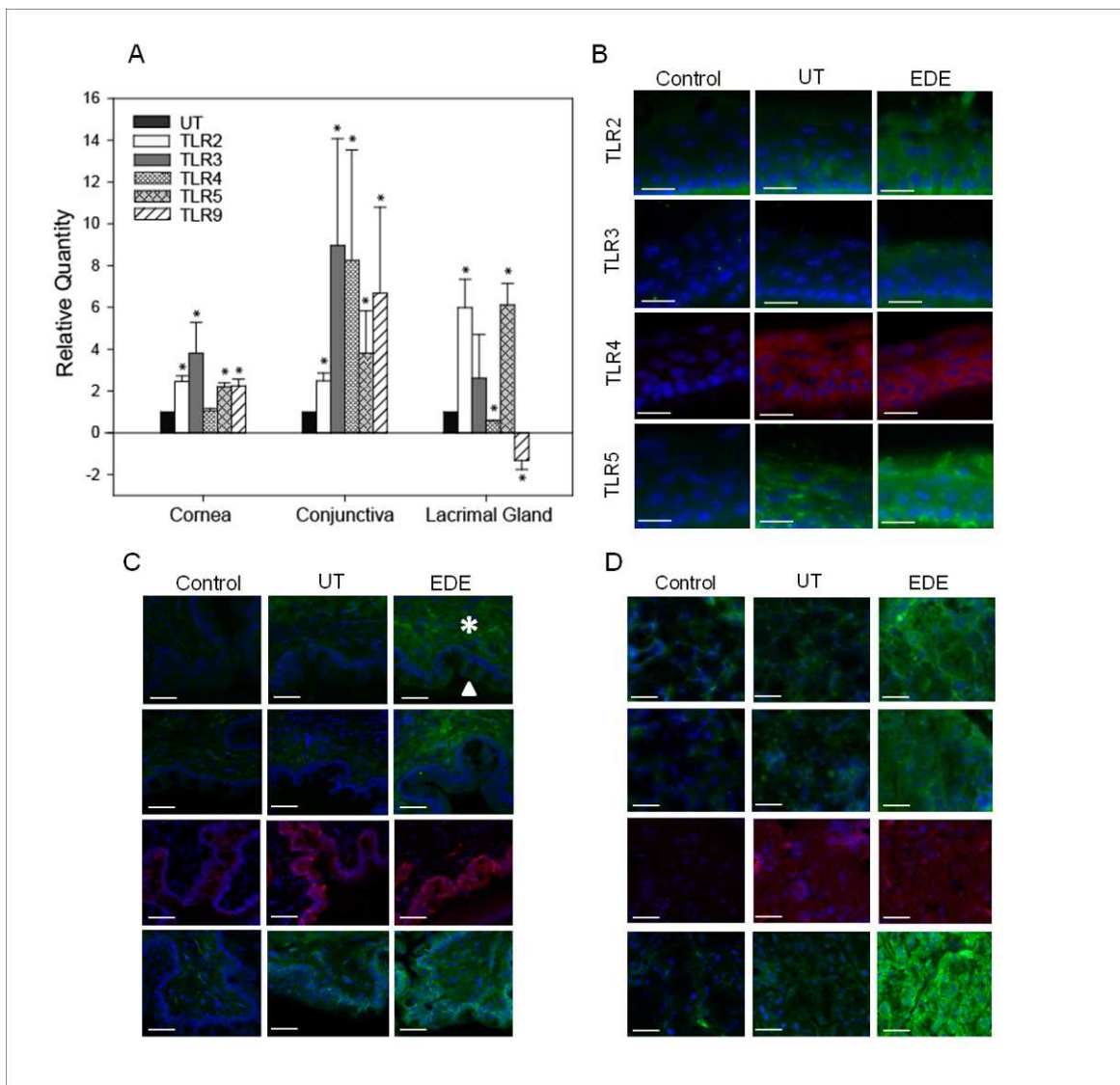


FIGURE 1. Toll-like receptor mRNA and protein expression on the ocular surface and lacrimal gland in mice with and without EDE. Corneal epithelial, conjunctival, and lacrimal gland TLR2, 3, 4, 5, and TLR9 mRNA expression was compared among mice subjected to EDE for 5 days and UT controls (A). *P* less than or equal to 0.05 was considered to be significant (*) by Student's *t*-test. The data are from three independent experiments and are the mean \pm SD. TLR2-5 protein was compared between mice with EDE and UT in the cornea (B), palpebral conjunctiva (C), and lacrimal gland (D). The controls include untreated animals and isotype matched nonspecific antibodies (control). *Arrow* and *asterisk* indicate conjunctiva epithelium and substantia propia, respectively (C). Data are representative of two independent experiments. Blue fluorescent DAPI stained the cell nuclei. All images were taken at 200 \times magnification. *Scale bar* represents 20 (B) or 40 (C-D) μ m.

epithelium in mice with EDE (Fig. 1). Immunostaining revealed that TLR agonist cocktail treatment decreased the expression of mBD-4 but had little effect on mBD-3 and CRAMP after 24 hours (Fig. 2C).

Clinical Objective Measurements and hCAP-18, hBD-2, TLR4, TLR5, and TLR9 mRNA Expression in Dry Eye Subjects

All DTS syndrome patients (*n* = 5) had significantly worse clinical objective findings than healthy control subjects (*n* = 4), except for corneal staining (Fig. 3A). One way ANOVA revealed a statistically significant difference in AMPs expression between healthy and dry eye subjects $F(2, 1163)$ equals 9.696, *P* = 0.003. DTS subjects had significant decrease in TLR9

mRNA to 0.13 ± 0.22 , while TLR4 was increased by 1.66 ± 1.3 -fold, but the latter did not achieve statistical significance. There was no change in TLR5 and hCAP-18 (LL-37) mRNA expression, while hBD-2 mRNA was significantly increased by 19.8 ± 13.2 -fold compared with age- and sex-matched healthy subjects (Fig. 3B). Of all the clinical objective measurements, there was a significant correlation only between an increase in hBD-2 mRNA expression and corneal staining (*P* = 0.048, R^2 = 0.81) in DTS patients (Fig. 3C).

Mice with EDE Have Significantly Increased Fluorescein Staining

Images of untreated mice (*n* = 6) revealed little corneal staining compared with the EDE mice (*n* = 8, Fig. 4A). To

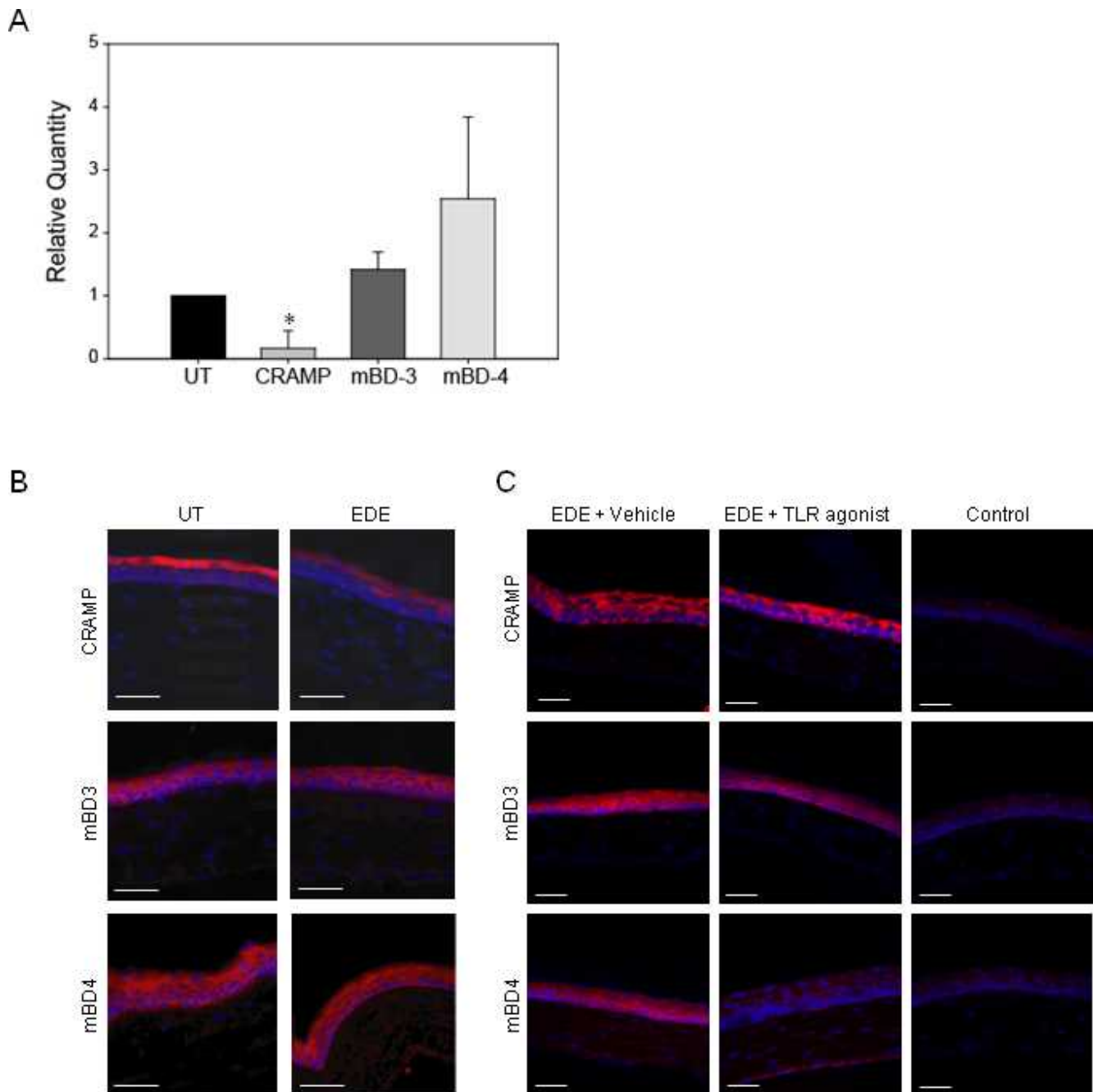


FIGURE 2. EDE and TLR activation modulate the expression of AMPs on the ocular surface. mRNA and protein expression of mBD-3, mBD-4, and CRAMP was compared among UT mice and mice with EDE by RT-PCR, n equals 3 (**A**) with P less than or equal to 0.05 considered to be significant (*) by Student's t -test, and by immunostaining, n equals 3 (**B**). In a separate experiment, mice were subjected to EDE and then a one-time topical application of either agonist cocktail for TLR2, 3, 5, and 9 or the endotoxin-free vehicle control. AMP expression was then examined by immunostaining 24 hours later (**C**). Blue fluorescent DAPI stained the cell nuclei. Some slides were incubated with the respective isotype antibody (control). All images were taken at 200 \times magnification. Scale bar represents 40 μ m.

quantify the staining pattern, ImageJ analysis was performed and revealed significantly more fluorescein staining (OD: 8281.7 ± 3451.5 , OS: $10,458.5 \pm 4735.5$) in mice with 5D EDE compared with UT control mice (OD: 85.0 ± 156.4 , OS: 280.8 ± 205.1) when comparing the same eye between the two groups (UT OD to EDE OD) as shown in Figure 4B. There was no significant difference between TLR agonist and vehicle treated samples.

TLR Agonist Increased the Recruitment of Inflammatory Cells into the Anterior Stroma in Mice with a Corneal Scratch but Not EDE

In the positive control scratch model, enface images revealed TLR agonist treatment increased the recruitment of inflammatory cells into the anterior stroma compared with the fellow eye which received the scratch and vehicle control (Fig. 5A).

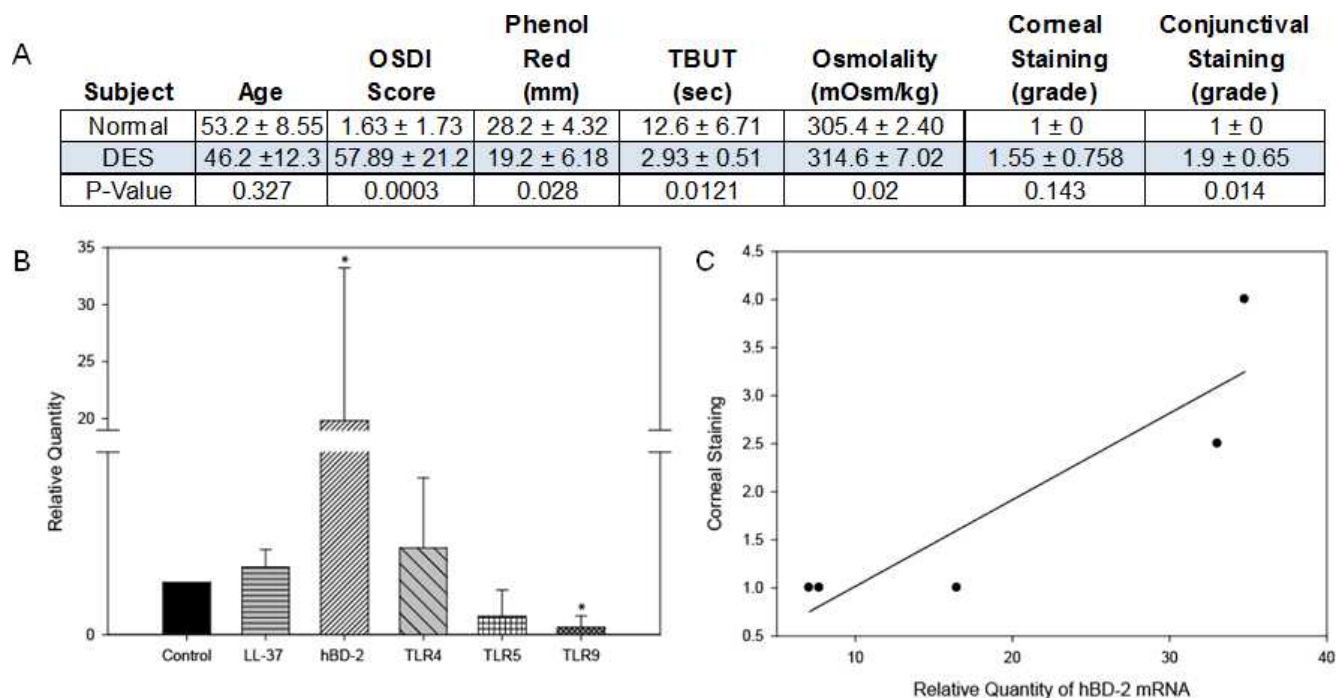


FIGURE 3. Clinical objective measurements and AMP and TLR mRNA expression in subjects with DTS syndrome and age/sex-matched subjects. Subjects were classified as having DTS based on their subjective responses to the OSDI questionnaire and clinical objective measurements (A). CIC samples were analyzed to compare hCAP-18 (LL-37 precursor), hBD-2, TLR4, TLR5, and TLR9 mRNA expression by RT-PCR (B). The correlation between hBD-2 mRNA expression and corneal staining in DTS patients was determined (C). *P* less than or equal to 0.05 was considered to be significant (*) by Student's *t*-test. The data are representative of five DTS and four control subjects.

Oblique cross-sections confirmed that inflammatory cells were localized to the anterior half of the stroma (Fig. 5B). However, in UT and EDE mice, TLR agonist topical treatment did not recruit significant numbers of inflammatory cells into the stroma.

TLR Agonists Modulate the CCT in Mice with EDE and Corneal Scratch

Central corneal cross-sectional images revealed that only in EDE mice, six of eight (75%) eyes treated with the topical TLR

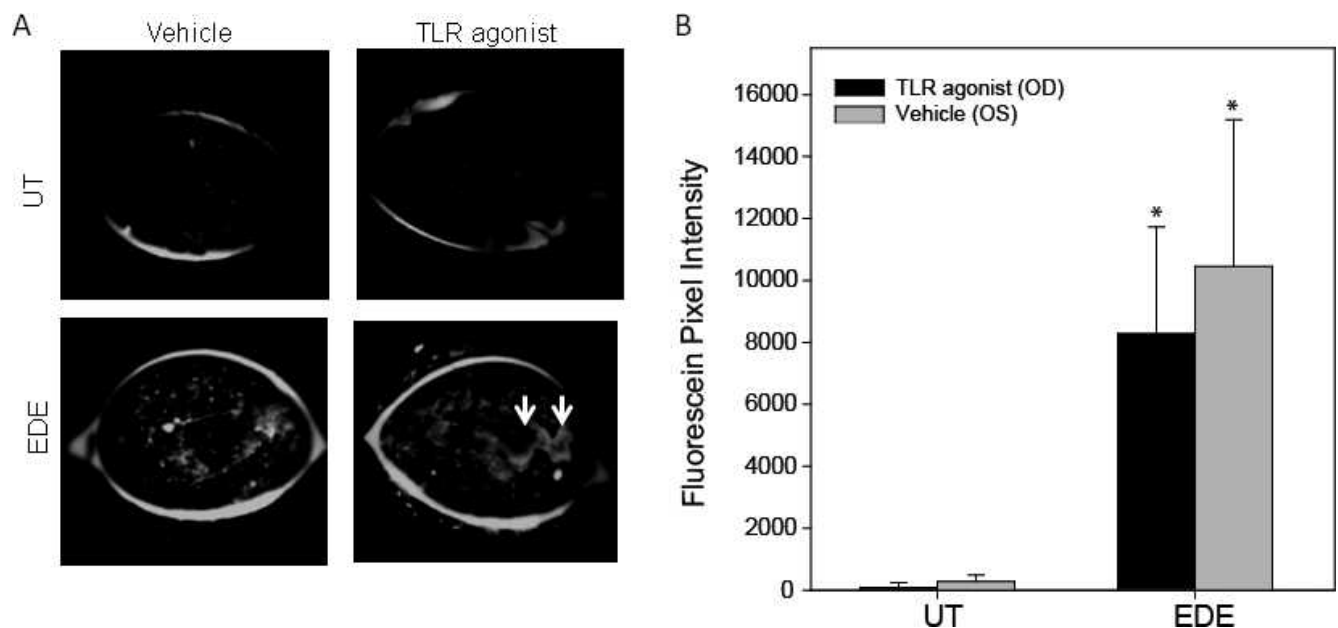


FIGURE 4. Mice with EDE have significantly increased fluorescein staining compared with UT control mice. The Spectralis was used to evaluate the corneal epithelial integrity in UT (*n* = 6) mice and mice subjected to EDE (*n* = 8). Following treatment, mice were anesthetized and corneal staining was examined using a 488 nm wavelength blue light illumination (A). White arrows indicate areas of fluorescein pooling in large superficial defects. The pixel intensity was quantified (B) compared among UT and EDE mice (e.g., UT OD versus EDE OD). *P* less than or equal to 0.05 was considered to be significant (*) by Student's *t*-test.

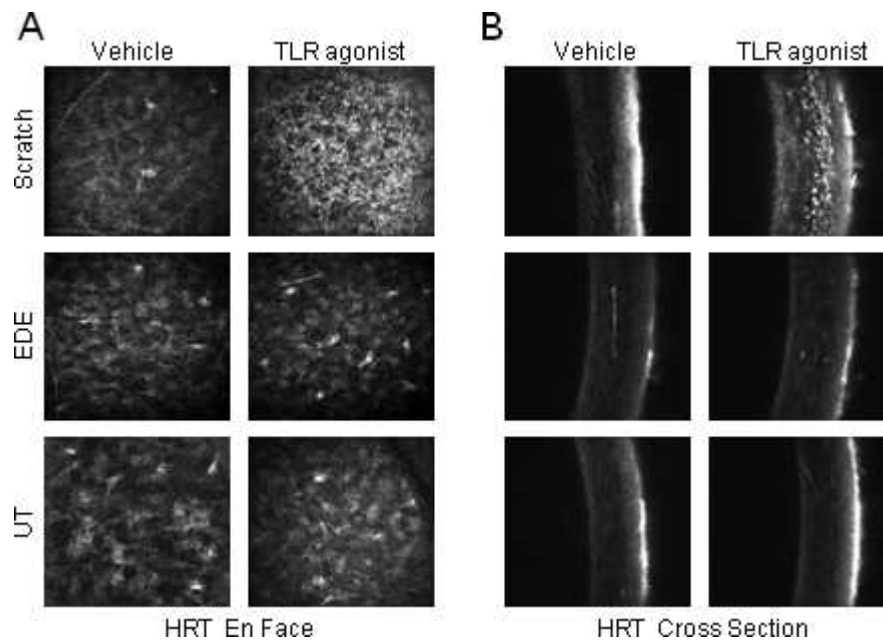


FIGURE 5. TLR agonist increases the recruitment of inflammatory cells into the anterior stroma in mice with a corneal scratch but not EDE. TLR agonist cocktail and the vehicle control were applied to the right and left eye, respectively, of the scratched ($n = 3$), UT ($n = 6$), and EDE ($n = 8$) mice, then live in vivo enface images (A) and oblique cross-sections (B) were taken with the cornea module of the HRT III 24 hours later.

agonist had an epithelial defect compared with two of the eight (25%) left eyes that were given the vehicle control. Whereas none of the UT or the mice that were scratched 24 hours prior had central epithelial defects (Fig. 6A). CCT measurements revealed no significant difference in CCT between the TLR agonist treated (OD) and the vehicle control (OS) in the UT mice. However, in mice with EDE, TLR agonist treatment significantly decreased CCT by almost 24% compared with the vehicle control ($87.2 \pm 12.0 \mu\text{m}$ versus $114.1 \pm 10.3 \mu\text{m}$, Fig. 6B). In the positive control scratch model, TLR agonist treatment significantly increased CCT by $42.3 \mu\text{m}$. In this model the TLR agonist treated eye CCT averaged $165.6 \pm 13.9 \mu\text{m}$, whereas vehicle control treated eye CCT averaged $122.3 \pm 6.1 \mu\text{m}$. To further examine histologic changes that occur in the EDE mice following TLR agonist treatment, the eyes from the EDE mouse depicted in Figure 6A was paraffin processed and H&E stained. TLR agonist treatment revealed epithelial defects and stromal thinning (Fig. 6C).

DISCUSSION

The results of this study demonstrate that EDE modulates the expression of several TLRs on the ocular surface and lacrimal gland, and DTS modulates the expression of AMPs on the ocular surface in humans and the mouse model. Experimental dry eye increased TLR expression and further topical application of TLR agonist cocktail downregulated the expression of mBD-4 and resulted in a thinner cornea from corneal ulceration which may increase susceptibility to additional inflammation and microbial infections in dry eye.

Previous studies have shown that TLRs are increased in SS and DTS and it has been suggested that this may contribute to the inflammatory environment.^{17,18} In this study, we found that TLR2-5 and TLR9 were upregulated in the conjunctiva while TLR2, 3, 5, and 9, but not TLR4 were upregulated in the mouse corneal epithelium, which is in partial agreement with a previously published report showing that TLR5 mRNA expression is increased in the cornea of a SS mouse model

(Christopherson PL, et al. *IOVS* 2005;46:ARVO E-Abstract 4462). In agreement with our data, a recent report found that EDE did not increase TLR4 mRNA expression in the corneal epithelium.²⁵ However, using flow cytometry, a sensitive technique for quantifying changes in protein, the authors were able to detect EDE stimulated intracellular TLR4 to be expressed on the cell surface and also increased TLR4 expression in the corneal stroma, which was not examined in this present study.²⁵ In addition to this, they also reported²⁵ that TLR4 inhibition decreased the severity of dry eye corneal staining and significantly reduced the IL-1 β , IL-6, and TNF mRNA expression and infiltration of CD11b⁺ cells and MHC-II^{hi} CD11b⁺ cells into the cornea and lymph node, respectively.²⁵ To further support the role of TLR in DTS, we have previously shown TLR expression is modulated in the conjunctiva in dry eye subjects and in human ocular surface cells in response to dry eye associated conditions such as hyperosmolar stress and desiccation (Redfern RL, et al. *IOVS* 2007;48:ARVO E-Abstract 3651).

In the current study, EDE increased TLR expression on the ocular surface, and topical application of TLR agonists in EDE mice resulted in corneal ulceration and a significantly thinner central cornea by approximately 24%, which may be attributed to dehydration and/or physical disruption to the tissue, compared with the vehicle control. While the mechanism by which this occurs is unclear, one scenario envisioned is that TLR agonists activate the corneal epithelium to stimulate the production of additional MMPs that further disrupts the compromised EDE ocular surface. In support of this a recent report found that in human corneal epithelial cells, TLR2 agonist treatment upregulated MMP-1 and -9 expression,²⁶ and we have found that TLR6/2, 3, and 5 agonists increase MMP-9 mRNA expression and protein levels (Redfern RL, unpublished observations, 2012). These findings suggest that TLR activation on the compromised ocular surface, potentially by endogenous stress ligands or microbes stimulates MMP production, which may exacerbate dry eye inflammation and destruction.

EDE was also found to significantly reduce the expression of CRAMP in the corneal epithelium, which may predispose mice to microbial infections. In support of this, CRAMP knockout

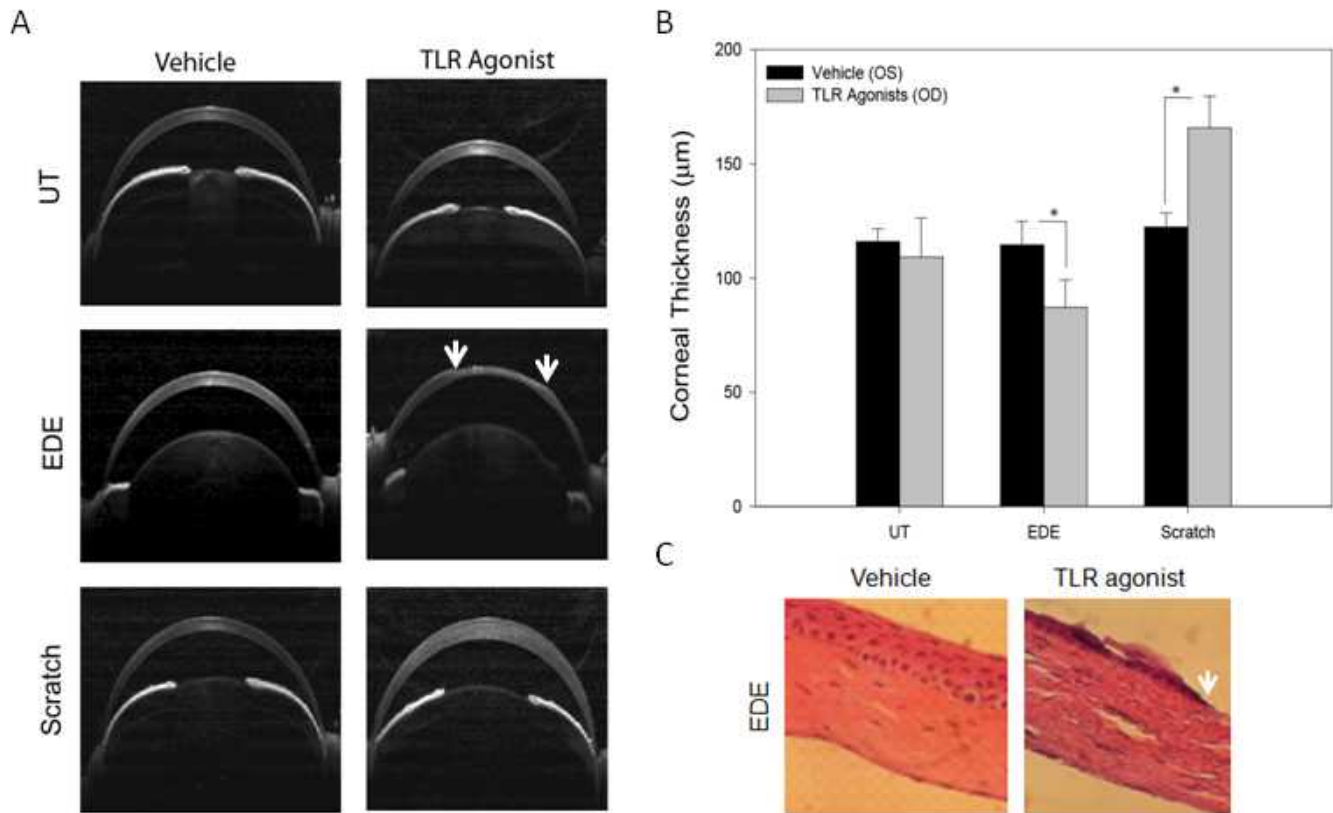


FIGURE 6. TLR agonist modulates the central corneal thickness in mice with EDE and corneal scratch. Cross-sectional images (A) and measurements (B) were obtained from agonist treated mice by selecting the scan which passed through the center of the pupil with the iris plane perpendicular to the scanning beam. Using ImageJ three CCT measurements were made on each scan, one at the center and one 50 μm to the right and left of center and averaged. P less than or equal to 0.05 was considered to be significant (*) by Student's t -test. Eyes from the EDE mouse depicted in (A) were paraffin processed and H&E stained. TLR agonist treated corneas revealed epithelial thinning and epithelial and stromal defects (C). All H&E images in were taken at 100 \times magnification. White arrows are suggestive of areas of epithelial loss.

mice are more susceptible to *Pseudomonas aeruginosa*²⁰ and *Candida albicans*²⁷ keratitis, as these animals have significant delayed bacterial clearance and an increased number of infiltrating neutrophils in the cornea. An increase severity of *P. aeruginosa* infection has also been observed in BALB/c mice when mBD-2 and/or mBD-3 are significantly reduced by siRNA.^{28,29} However, interestingly and relevant to the present study, a recent report has shown that C57BL/6 EDE mice subjected to a high inoculum of either an invasive (strain PA01) or cytotoxic (strain 6206) strain of *P. aeruginosa* had enhanced bacterial clearance and did not have an increase susceptibility to infection despite decreased tear volume (Heimer SR, et al. *IOVS* 2010;51:ARVO E-Abstract 3897). The lack of susceptibility to *P. aeruginosa* infection may be a result of an insufficient disruption of the ocular surface since the authors' report no corneal fluorescein staining in the mice EDE, suggesting their model was not as severe as the one used in this study. Alternatively, studies are suggesting that enhanced innate immune mechanisms may protect the dry eye from invading pathogens. For example, secreted phospholipase A2 (sPLA2) binds bacterial surfaces kills via its phospholipolytic enzymatic activity.^{30,31} The ocular surface has increased levels and activity of sPLA2 in tear fluid of dry eye patients,^{32,33} suggesting a potential role in reducing the risk for microbial infections at the ocular surface in dry eye patients.

In this current study using a small number of DTS subjects, conjunctival impression cytology samples revealed a significant decrease in TLR9, which occurred in the lacrimal gland in the EDE mouse model. As with the conjunctival tissue from EDE

mice, TLR4 mRNA was increased in CIC samples from DTS patients, although this change was modest at most. There was a significant increase in hBD-2 mRNA in DTS patients, which was significantly correlated with corneal staining. Previous studies have shown that in the re-epithelializing cornea, there is an increase in hBD-2¹² and IL-1¹³ with IL-1 capable of inducing hBD-2 expression.¹³ Considering this, corneal epithelial defects may increase IL-1 production and account for the increase in hBD-2 on the ocular surface of DTS patients. In mice with EDE, there was also an increase in mBD-3 and -4 (orthologue to hBD-2) but this was not statistically significant. Suggesting that in the EDE mouse, baseline levels of mBD-3 and -4 maybe sufficient in protecting the ocular surface when compromised from EDE. Another scenario envisioned is that other antimicrobial peptides, not examined in this study, may provide protection against infection during DTS, but little data exists in the literature regarding this area.

The human corneal epithelium normally expresses hBD-1 and -3, and low levels of LL-37, which may provide baseline protection against pathogens. We previously found that hBD-2, but not hBD-1 and -3, were increased in subjects with DTS, while LL-37 expression was not examined.³⁴ In addition to this, mBD-2 (homologue to hBD-1) was downregulated to undetectable levels in mice with EDE, whereas there was no change in mBD-1 (homologue to hBD-1) expression.³⁵ LL-37 is constitutively expressed on the ocular surface, and like hBD-2, its expression is upregulated during inflammatory conditions, such as wound healing, whereas hBD-1 and -3 are not.^{12,36} Considering this, it seemed logical that both hBD-2 and LL-37

would be upregulated in subjects with DTS when the ocular surface is most likely to be compromised; however, this was not found in the current study. A new novel AMP, DEFB109 that is constitutively expressed on the ocular surface has been shown to be downregulated in subjects with DTS and also in subjects with ocular microbial infections,⁵⁷ suggesting that a balance in AMP expression occurs when the ocular surface becomes inflamed. This same scenario might be true for mBD-4 when extensive inflammation occurs. In the EDE, a severe form of DTS occurs and when TLR agonists are applied to the already inflamed ocular surface, mBD-4 expression is dampened.

These findings demonstrate that the expression of antimicrobial peptides and TLRs on the ocular surface are modulated during EDE. This enhanced expression may provide the ocular surface with additional protection against potential pathogens when the ocular surface is vulnerable. However TLR activation on the ocular surface may also have deleterious effects, as TLR activation in EDE mice promoted cornea epithelial ulceration a sign of severe dry eye, suggesting a potential mechanism for ocular surface destruction in dry eye.

Acknowledgments

The authors thank Cintia De Paiva and Solherny Pangelinan for their assistance with the experimental dry eye mouse model and the subjects who participated in this study.

References

- Miljanovic B, Dana R, Sullivan DA, Schaumberg DA. Impact of dry eye syndrome on vision-related quality of life. *Am J Ophthalmol*. 2007;143:409–415.
- Gilbard JP, Farris RL, Santamaria J II. Osmolarity of tear microvolumes in keratoconjunctivitis sicca. *Arch Ophthalmol*. 1978;96:677–681.
- Farris RL. Tear osmolarity—a new gold standard? *Adv Exp Med Biol*. 1994;350:495–503.
- Bron AJ, Tiffany JM, Yokoi N, Gouveia SM. Using osmolarity to diagnose dry eye: a compartmental hypothesis and review of our assumptions. *Adv Exp Med Biol*. 2002;506:1087–1095.
- Afonso AA, Sobrin L, Monroy DC, Selzer M, Lokeshwar B, Pflugfelder SC. Tear fluid gelatinase B activity correlates with IL-1 α concentration and fluorescein clearance in ocular rosacea. *Invest Ophthalmol Vis Sci*. 1999;40:2506–2512.
- Pflugfelder SC, Jones D, Ji Z, Afonso A, Monroy D. Altered cytokine balance in the tear fluid and conjunctiva of patients with Sjogren's syndrome keratoconjunctivitis sicca. *Curr Eye Res*. 1999;19:201–211.
- Solomon A, Dursun D, Liu Z, Xie Y, Macri A, Pflugfelder SC. Pro- and anti-inflammatory forms of interleukin-1 in the tear fluid and conjunctiva of patients with dry-eye disease. *Invest Ophthalmol Vis Sci*. 2001;42:2283–2292.
- Luo L, Li DQ, Doshi A, Farley W, Corrales RM, Pflugfelder SC. Experimental dry eye stimulates production of inflammatory cytokines and MMP-9 and activates MAPK signaling pathways on the ocular surface. *Invest Ophthalmol Vis Sci*. 2004;45:4293–4301.
- Vivino FB, Minerva P, Huang CH, Orlin SE. Corneal melt as the initial presentation of primary Sjogren's syndrome. *J Rheumatol*. 2001;28:379–382.
- Derk CT, Vivino FB. A primary care approach to Sjogren's syndrome. Helping patients cope with sicca symptoms, extraglandular manifestations. *Postgrad Med*. 2004;116:49–54.
- Gordon YJ, Huang LC, Romanowski EG, Yates KA, Proske RJ, McDermott AM. Human cathelicidin (LL-37), a multifunctional peptide, is expressed by ocular surface epithelia and has potent antibacterial and antiviral activity. *Curr Eye Res*. 2005;30:385–394.
- McDermott AM, Redfern RL, Zhang B. Human beta-defensin 2 is up-regulated during re-epithelialization of the cornea. *Curr Eye Res*. 2001;22:64–67.
- McDermott AM, Redfern RL, Zhang B, Pei Y, Huang L, Proske RJ. Defensin expression by the cornea: multiple signalling pathways mediate IL-1 β stimulation of hBD-2 expression by human corneal epithelial cells. *Invest Ophthalmol Vis Sci*. 2003;44:1859–1865.
- McNamara NA, Van R, Tuchin OS, Fleiszig SM. Ocular surface epithelia express mRNA for human beta defensin-2. *Exp Eye Res*. 1999;69:483–490.
- Redfern RL, Reins RY, McDermott AM. Toll-like receptor activation modulates antimicrobial peptide expression by ocular surface cells. *Exp Eye Res*. 2011;92:209–220.
- Johnson AC, Heinzel FP, Diaconu E, et al. Activation of toll-like receptor (TLR) 2, TLR4, and TLR9 in the mammalian cornea induces MyD88-dependent corneal inflammation. *Invest Ophthalmol Vis Sci*. 2005;46:589–595.
- Spachidou MP, Bourazopoulou E, Maratheftis CI, et al. Expression of functional Toll-like receptors by salivary gland epithelial cells: increased mRNA expression in cells derived from patients with primary Sjogren's syndrome. *Clin Exp Immunol*. 2007;147:497–503.
- Kawakami A, Nakashima K, Tamai M, et al. Toll-like receptor in salivary glands from patients with Sjogren's syndrome: functional analysis by human salivary gland cell line. *J Rheumatol*. 2007;34:1019–1026.
- De Paiva CS, Chotikavanich S, Pangelinan SB, et al. IL-17 disrupts corneal barrier following desiccating stress. *Mucosal Immunol*. 2009;2:243–253.
- Huang LC, Redfern RL, Narayanan S, Reins RY, McDermott AM. In vitro activity of human beta-defensin 2 against *Pseudomonas aeruginosa* in the presence of tear fluid. *Antimicrob Agents Chemother*. 2007;51:3853–3860.
- Schiffman RM, Christianson MD, Jacobsen G, Hirsch JD, Reis BL. Reliability and validity of the Ocular Surface Disease Index. *Arch Ophthalmol*. 2000;118:615–621.
- Hanlon SD, Patel NB, Burns AR. Assessment of postnatal corneal development in the C57BL/6 mouse using spectral domain optical coherence tomography and microwave-assisted histology. *Exp Eye Res*. 2011;93:363–370.
- Labbe A, Liang H, Martin C, Brignole-Baudouin F, Warnet JM, Baudouin C. Comparative anatomy of laboratory animal corneas with a new-generation high-resolution in vivo confocal microscope. *Curr Eye Res*. 2006;31:501–509.
- Reichard M, Hovakimyan M, Wree A, et al. Comparative in vivo confocal microscopical study of the cornea anatomy of different laboratory animals. *Curr Eye Res*. 2010;35:1072–1080.
- Lee HS, Hattori T, Park EY, Stevenson W, Chauhan SK, Dana R. Expression of toll-like receptor (TLR) 4 contributes to corneal inflammation in experimental dry eye disease. *Invest Ophthalmol Vis Sci*. 2012;53:5632–5640.
- Li DQ, Zhou N, Zhang L, Ma P, Pflugfelder SC. Suppressive effects of azithromycin on zymosan-induced production of proinflammatory mediators by human corneal epithelial cells. *Invest Ophthalmol Vis Sci*. 2010;51:5623–5629.
- Gao N, Kumar A, Guo H, Wu X, Wheeler M, Yu FS. Topical flagellin-mediated innate defense against *Candida albicans* keratitis. *Invest Ophthalmol Vis Sci*. 2011;52:3074–3082.
- Wu M, McClellan SA, Barrett RP, Hazlett LD. Beta-defensin-2 promotes resistance against infection with *P. aeruginosa*. *J Immunol*. 2009;182:1609–1616.

29. Wu M, McClellan SA, Barrett RP, Zhang Y, Hazlett LD. Beta-defensins 2 and 3 together promote resistance to *Pseudomonas aeruginosa* keratitis. *J Immunol*. 2009;183:8054-8060.
30. Buckland AG, Wilton DC. The antibacterial properties of secreted phospholipases A(2). *Biochim Biophys Acta*. 2000;1488:71-82.
31. Nevalainen TJ, Graham GG, Scott KF. Antibacterial actions of secreted phospholipases A2. Review. *Biochim Biophys Acta*. 2008;1781:1-9.
32. Wei Y, Epstein SP, Fukuoka S, Birmingham NP, Li XM, Asbell PA. sPLA2-IIa amplifies ocular surface inflammation in the experimental dry eye (DE) BALB/c mouse model. *Invest Ophthalmol Vis Sci*. 2011;52:4780-4788.
33. Aho V, Nevalainen T, Saari M. Group IIA phospholipase A2 content of tears in patients with keratoconjunctivitis sicca. *Graefes Arch Clin Exp Ophthalmol*. 2002;40:521-523.
34. Narayanan S, Miller WL, McDermott AM. Expression of human beta-defensins in conjunctival epithelium: relevance to dry eye disease. *Invest Ophthalmol Vis Sci*. 2003;44:3795-3801.
35. Narayanan S, Corrales RM, Farley W, McDermott AM, Pflugfelder SC. Interleukin-1 receptor-1-deficient mice show attenuated production of ocular surface inflammatory cytokines in experimental dry eye. *Cornea*. 2008;27:811-817.
36. Huang LC, Petkova TD, Reins RY, Proske RJ, McDermott AM. Multifunctional roles of human cathelicidin (LL-37) at the ocular surface. *Invest Ophthalmol Vis Sci*. 2006;47:2369-2380.
37. Abedin A, Mohammed I, Hopkinson A, Dua HS. A novel antimicrobial peptide on the ocular surface shows decreased expression in inflammation and infection. *Invest Ophthalmol Vis Sci*. 2008;49:28-33.